Control of Barite Morphology by Double-Hydrophilic Block Copolymers

Limin Qi,* Helmut Cölfen, and Markus Antonietti

Max Planck Institute of Colloids and Interfaces, D-14424 Potsdam, Germany

Received March 17, 2000. Revised Manuscript Received May 2, 2000

Barite particles with a rich variety of well-defined morphologies have been synthesized by using double-hydrophilic block copolymers (which consist of a hydrophilic solvating block and a hydrophilic binding block) as crystal growth modifiers to direct the controlled precipitation of barium sulfate from aqueous solution. The influences of variation in functional group and molecular structure of the copolymers as well as variation of pH condition on the particle size and morphology were investigated. It was revealed that in the presence of copolymers containing carboxylic acid groups at a pH above 5, the obtained $BaSO_4$ particles always exhibit a nanocrystalline structure due to the large inhibition effect of the polyanionic chain on the barite crystallization. With decreasing pH, the particle size essentially increases, and the particle morphology generally varies from ovals through peanuts to peaches. In the presence of the phosphonated copolymer PEG-*b*-PMAA-PO_3H_2 at pH 5, large bundles of barite nanofilaments ranging from 20 to 30 nm in diameter, each of which is a single crystal elongated along the crystallographic [1$\bar{2}$0] axis, can be produced due to the strong and specific interaction between the phosphonate groups of the copolymer and the crystallizing $BaSO_4$ particles. The obtained results demonstrate the tremendous potential of double-hydrophilic block copolymers as tools for the controlled synthesis of inorganic crystals with unusual, well defined morphologies.

Introduction

The synthesis of inorganic materials of specific size and morphology is a key aspect in the development of new materials in fields as diverse as catalysis, medicine, electronics, ceramics, pigments, and cosmetics.[1–4] Compared with the size control, the morphology control has been much more difficult to achieve by means of classical colloid chemistry, although micrometer-sized colloidal particles with various shapes, such as spheres, needles, plates, cubes, and stars, can be obtained by the use of controlled precipitation conditions in combination with low molecular weight additives or salts.[5] Biological systems, on the other hand, use supramolecular assemblies of organized biopolymers (proteins and polysaccharides) to exert exquisite control over the processes of biomineralization, which results in unique biominerals (for example, coccoliths, seashells, bone, teeth, and many others) with their structure, size, and morphology regulated to optimally fit their functions as materials.[6,7] The strategy that organic templates with complex functionalization patterns are used to control the nucleation, growth, and alignment of inorganic crystals has been recently adapted for the biomimetic synthesis of inorganic materials with complex form.[1,8]

One major approach is to mimic natural biomineralization processes directly. For example, the protein macromolecules isolated from mollusk shells have been used for in vitro $CaCO_3$ mineralization experiments.[9–11] A designed peptide has been synthesized and used for the mineralization of calcite with controlled morphology.[12] In addition, collagen/gelatin matrixes have been used for the biomimetic crystallization of calcium carbonate[13,14] and the biomimetic growth and self-assembly of fluorapatite.[15] Another major approach to biomimetic synthesis is to just mimic the biomineralization principles, in which commercial surfactants or synthetic functional polymers are used as templates or crystal growth modifiers. Specifically, organized assemblies of surfactants, such as Langmuir monolayers,[16–19] have been used as effective templates for the control of crystal

(1) Mann, S.; Ozin, G. A. *Nature* **1996,** *382*, 313.
(2) Yang, H.; Coombs, N.; Ozin, G. A. *Nature* **1997,** *386*, 692.
(3) Ahmadi, T. S.; Wang, Z. L.; Green, T. C.; Henglein, A.; El-Sayed, M. A. *Science* **1996,** *272*, 1924.
(4) Matijevic, E. *Curr. Opin. Colloid Interface Sci.* **1996,** *1*, 176.
(5) Matijevic, E. *Chem. Mater.* **1993,** *5*, 412.
(6) Mann, S.; Webb, J.; Williams, R. J. P., Eds. *Biomineralization, Chemical and Biochemical Perspectives*; VCH: Weinheim, 1989.
(7) Mann, S. *Nature* **1993,** *365*, 499.

(8) Mann, S. *Biomimetic Materials Chemistry*; VCH: Weinheim, 1995.
(9) Falini, G.; Albeck, S.; Weiner, S.; Addadi, L. *Science* **1996,** *271*, 67.
(10) Levi, Y.; Albeck, S.; Brack, A.; Weiner, S.; Addadi, L. *Chem. Eur. J.* **1998,** *4*, 389.
(11) Belcher, A. M.; Wu, X. H.; Christensen, R. J.; Hansma, P. K.; Stucky, G. D.; Morse, D. E. *Nature* **1996,** *381*, 36.
(12) DeOliveira, D. B.; Laursen, R. A. *J. Am. Chem. Soc.* **1997,** *119*, 10627.
(13) Falini, G.; Fermani, S.; Gazzano, M.; Ripamonti, A. *Chem. Eur. J.* **1997,** *3*, 1807.
(14) Falini, G.; Fermani, S.; Gazzano, M.; Ripamonti, A. *Chem. Eur. J.* **1998,** *4*, 1048.
(15) (a) Kniep, R.; Busch, S. *Angew. Chem., Int. Ed. Engl.* **1996,** *35*, 22. (b) Busch, S.; Dolhaine, H.; DuChesne, A.; Heinz, S.; Hochrein, O.; Laeri, F.; Podebrad, O.; Vietze, U.; Weiland, T.; Kniep, R. *Eur. J. Inorg. Chem.* **1999,** 1643.
(16) Heywood, B. R.; Mann, S. *Adv. Mater.* **1994,** *6*, 9.
(17) Litvin, A. L.; Valiyaveettil, S.; Kaplan, D. L.; Mann, S. *Adv. Mater.* **1997,** *9*, 124.

nucleation and growth. On the other hand, soluble, low molecular weight or macromolecular additives have been shown to exert significant influence on the crystallization process.[20,21] However, the use of block copolymers as tools for the more subtle control of the inorganic crystallization, especially the control of the inorganic morphology, is just beginning to be explored.

Recently, it was shown that so-called double-hydrophilic block copolymers[22] can exert a strong influence on the external morphology and/or crystalline structure of inorganic particles such as calcium carbonate,[22–24] calcium phosphate,[25] and zinc oxide.[26] These copolymers consist of one hydrophilic block designed to interact strongly with the appropriate inorganic minerals and surfaces, and another hydrophilic block that does not exhibit strong interaction with the inorganic minerals or precursors and mainly promotes solubilization in water. Owing to the separation of the binding moiety and the solvating, noninteracting or weakly interacting moiety in such copolymers, complex patterns of chemical groups can be established by varying the binding and solvating blocks in the copolymers according to molecular design, resulting in operational crystal growth modifiers for the controlled mineralization. Moreover, the solution conditions such as pH can significantly influence the protonation degree of the interactive functional groups in copolymers as well as the molecular conformation of copolymers in solution, which could lead to even more operational possibilities.

Barium sulfate, commonly referred to as barite, has been widely used as a model system for the study of inorganic precipitation or crystallization. In addition to the application of barite as a filler of polymer materials and in pharmaceutical formulations, precipitation of barite is also of considerable industrial significance due to its tendency to form scale in off-shore oil wells. In recent years, some investigations on the organic template-directed barite crystallization have been reported. For example, Langmuir monolayers have been used as templates to direct the oriented nucleation and growth of barite,[27,28] whereas reverse micelles and microemulsions have been used as templates for the synthesis of barite nanoparticles and nanofilaments.[29,30] On the other hand, several kinds of organic additives have been used as crystal modifiers to direct the nucleation and growth of barite from aqueous solution.[20,31–33] In a recent letter, we demonstrated that barite with a variety of unusual, well-defined morphologies can be obtained via the controlled crystallization in the presence of double-hydrophilic block copolymers.[34] Here we describe the control of barite morphology using such copolymers in detail. The influences of variation in functional group and molecular structure of the copolymers as well as variation of the pH conditions on the morphology of the obtained barite particles were examined.

Experimental Section

Materials. Unless otherwise stated, all chemicals were obtained from Aldrich and used without further purification. Homopolymers poly(ethylene glycol) monomethyl ether (PEG, MW = 5000 g/mol) and poly(methacrylic acid, sodium salt) (PMAA, MW = 6500 g/mol) were purchased from Polysciences and Aldrich, respectively. A commercial block copolymer poly-(ethylene glycol)-*block*-poly(methacrylic acid) (PEG-*b*-PMAA, PEG = 3000 g/mol, PMAA = 700 g/mol) was obtained from Th. Goldschmidt AG, Essen, Germany. The carboxylic acid groups of this copolymer were partially amidated with aspartic acid (27%) to yield a polymer with amino acid side chains, PEG-*b*-PMAA-Asp, and were partially monophosphonated (21%) to give a copolymer with phosphonate groups, PEG-*b*-PMAA-PO$_3$H$_2$, respectively.[23] A block copolymer containing a poly(ethylenediaminetetraacetic acid) (EDTA)-like carboxy-functionalized block, poly(ethylene glycol)-*block*-poly(ethylene imine)-poly(acetic acid) (PEG-*b*-PEIPA, PEG = 5000 g/mol, PEIPA = 1800 g/mol) was synthesized as described elsewhere.[22] For the barite crystallization experiments, all copolymers were purified by exhaustive dialysis.

Barite Crystallization. The precipitation of BaSO$_4$ in the presence of various additives was carried out in a double jet reactor[23] thermostated at 25 °C. A solution of 300 mg of additives (either inorganic additives such as NH$_4$OH and HAc, or polymeric additives) in 300 mL of distilled water was adjusted to a desired pH using 1 M NaOH or HCl before it was used for the precipitation of BaSO$_4$. Under vigorous stirring, 0.5 M Ba(Ac)$_2$ and 0.5 M (NH$_4$)$_2$SO$_4$ were injected via capillaries into the reaction vessel with a reactant supply of 0.5 mL/h, which gave a BaSO$_4$ formation rate of 1.39×10^{-5} M/min. The reactant supply was stopped when the solution became obviously turbid or macroscopic crystal formation could be observed, i.e., the onset of BaSO$_4$ precipitation was reached; however, the injection under stirring was continued for at least 30 min in any case. The precipitates were left to stand in their mother solutions for at least 24 h to ensure complete equilibration.

Characterization. The resulting BaSO$_4$ precipitates were characterized by scanning electron microscopy (SEM) on a DSM 940 A (Carl Zeiss, Jena) microscope, and by transmission electron microscopy (TEM) with a Zeiss EM 912 Omega microscope. Thin-section samples (∼50 nm in width) for TEM were prepared by polymerization in epoxy resin and then were cut with an ultramicrotome. Dry powder samples were used for the measurements of X-ray powder diffraction (XRD) using a PDS 120 (Nonius GmbH, Solingen) with Cu Kα radiation, and thermogravimetry (TG) on a Netzsch TG 209 unit. The obtained XRD patterns were indexed with reference to the unit cell of the barite structure (a = 8.87 Å, b = 5.45 Å, c = 7.15 Å, space group *Pnma*).[35] The crystallite size of the obtained BaSO$_4$ particles was estimated from the half-height width of the barite (211) peak according to the Scherrer equation.

(18) Lahiri, J.; Xu, G.; Dabbs, D. M.; Yao, N.; Aksay, I. A.; Groves, J. T. *J. Am. Chem. Soc.* **1997**, *119*, 5449.

(19) Li, B.; Liu, Y.; Yu, J.; Bai, Y.; Pang, W.; Xu, R. *Langmuir*, **1999**, *15*, 4837.

(20) Davey, R. J.; Black, S. N.; Bromley, L. A.; Cotter, D.; Dobbs, B.; Rout, J. E. *Nature* **1991**, *353*, 549.

(21) Didymus, J. M.; Oliver, P.; Mann, S.; DeVries, A. L.; Hauschka, P. V.; Westbroek, P. *J. Chem. Soc., Faraday Trans.* **1993**, *89*, 2891.

(22) Sedlak, M.; Antonietti, M.; Cölfen, H. *Macromol. Chem. Phys.* **1998**, *199*, 247.

(23) Cölfen, H.; Antonietti, M. *Langmuir* **1998**, *14*, 582.

(24) Marentette, J. M.; Norwig, J.; Stockelmann, E.; Meyer, W. H.; Wegner, G. *Adv. Mater.* **1997**, *9*, 647.

(25) Antonietti, M.; Breulmann, M.; Göltner, C. G.; Cölfen, H.; Wong, K. K.; Walsh, D.; Mann, S. *Chem. Eur. J.* **1998**, *4*, 2493.

(26) Oner, M.; Norwig, J.; Meyer, W. H.; Wegner, G. *Chem. Mater.* **1998**, *10*, 460.

(27) Heywood, B. R.; Mann, S. *J. Am. Chem. Soc.* **1992**, *114*, 4681.

(28) Heywood, B. R.; Mann, S. *Langmuir* **1992**, *8*, 1492.

(29) Qi, L.; Ma, J.; Cheng, H.; Zhao, Z. *Colloids Surf. A* **1996**, *108*, 117.

(30) Hopwood, J. D.; Mann, S. *Chem. Mater.* **1997**, *9*, 1819.

(31) Bromley, L. A.; Cottier, D.; Davey, R. J.; Dobbs, B.; Smith, S.; Heywood, B. R. *Langmuir* **1993**, *9*, 3594.

(32) Benton, W. J.; Collins, I. R.; Grimsey, I. M.; Parkinson, G. M.; Rodger, S. A. *Faraday Discuss.* **1993**, *95*, 281.

(33) Rohl, A. L.; Gay, D. H.; Davey, R. J.; Catlow, C. R. A. *J. Am. Chem. Soc.* **1996**, *118*, 642.

(34) Qi, L.; Cölfen, H.; Antonietti, M. *Angew. Chem., Int. Ed.* **2000**, *39*, 604.

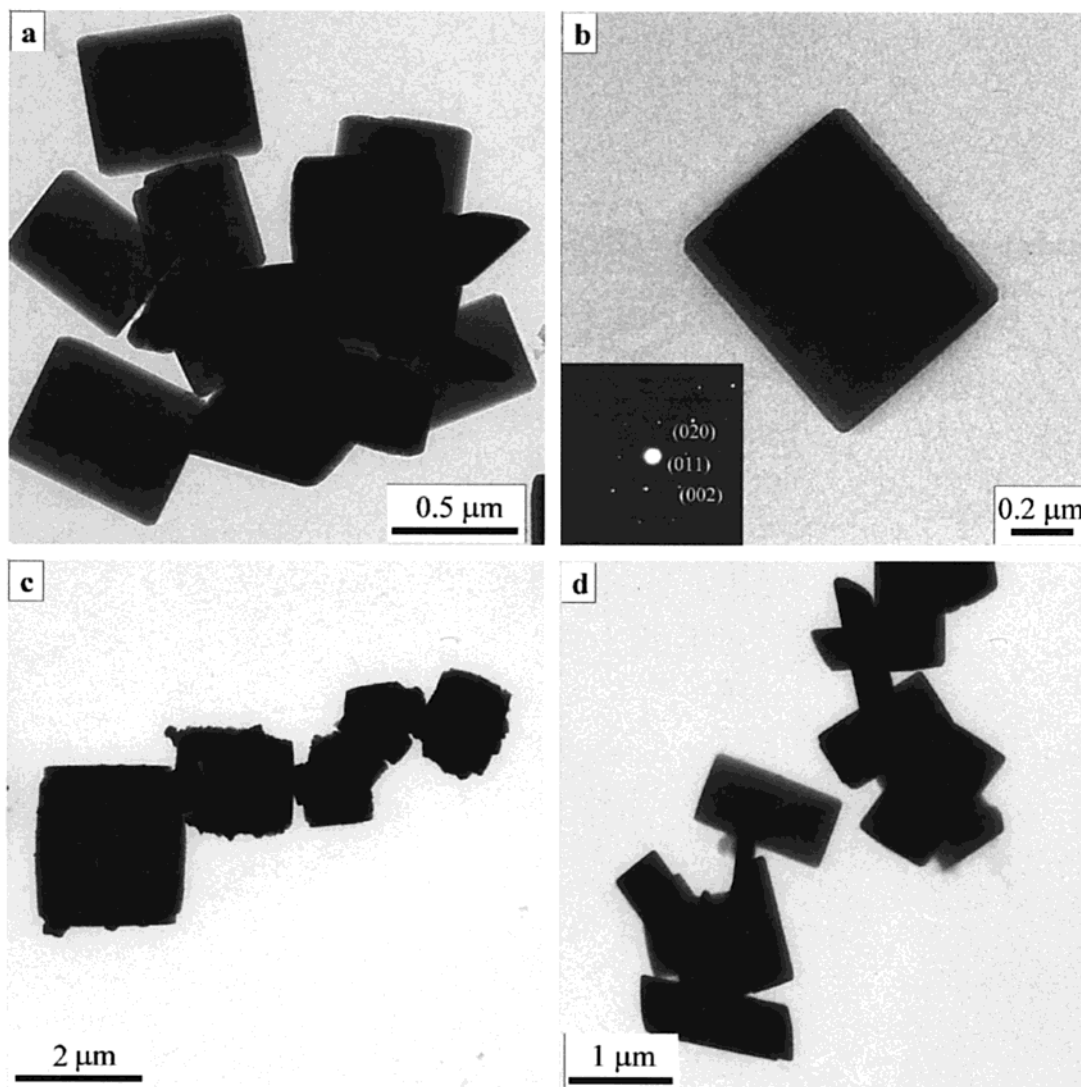(35) Pina, C. M.; Becker, U.; Risthaus, P.; Bosbach, D.; Putnis, A. *Nature* **1998**, *395*, 483.

Figure 1. TEM micrographs of BaSO$_4$ particles obtained in the presence of no additives at pH 7 (a, b), NH$_4$OH−NH$_4$Cl at pH 9 (c), and HAc−NaAc at pH 5 (d). Inset in (b) shows the associated single-crystal electron diffraction pattern, which corresponds to the [100] zone of barite.

Results and Discussion

Barite Crystallization in the Absence of Polymeric Additives. In the absence of polymeric additives, the precipitation process of BaSO$_4$ at different pH values was similar and the solution always became turbid in less than 30 min. All of the obtained products were revealed to be well-crystallized barite crystals according to the corresponding XRD results. As shown in Figure 1a, the barite crystals obtained in the absence of additives at pH 7 exhibit rectangular tablets with an average length of about 0.6 μm and a mean aspect ratio (*r*) of 1.2. Single-crystal electron diffraction patterns obtained from individual tablets indicate that they are single crystals elongated along the crystallographic [001] axis and are terminated by well-defined (001) faces (Figure 1b). Similar rectangular tablets with a mean length of 3.7 μm have were obtained from BaSO$_4$ supersaturated solution under static growth conditions.[27] However, the barite tablets obtained here are considerably smaller, presumably due to the double jet precipitation process that promotes the nucleation process, resulting in a larger number of smaller crystals.

Rectangular tablets of barite crystals can also be obtained in the presence of either NH$_4$OH−NH$_4$Cl (pH 9) or HAc−NaAc (pH 5) buffer solution. However, the product at pH 9 seems to exhibit somewhat rough edges and more severe aggregation. On the other hand, the product at pH 5 exhibits regularly rectangular tablets with relatively uniform size. The average length of the tablets is 1.2 μm with an aspect ratio of 1.5. It can be deduced that the addition of simple inorganic ions such as NH$_4^+$, Na$^+$, Ac$^-$, and Cl$^-$ together with pH variation between 9 and 5 does not show significant influence on the morphology of barite crystals under the present experimental conditions.

Barite Crystallization in the Presence of Homopolymers. PEG is a homopolymer without functional groups that can potentially interact with normal inorganic minerals. It has been reported that the addition of such homopolymers had no effect on the crystal morphologies of both CaCO$_3$ [24] and ZnO.[26] In the present case, the presence of PEG has not considerably delayed the onset of BaSO$_4$ precipitation at both pH 9 and pH 5, and the corresponding XRD results also suggest that
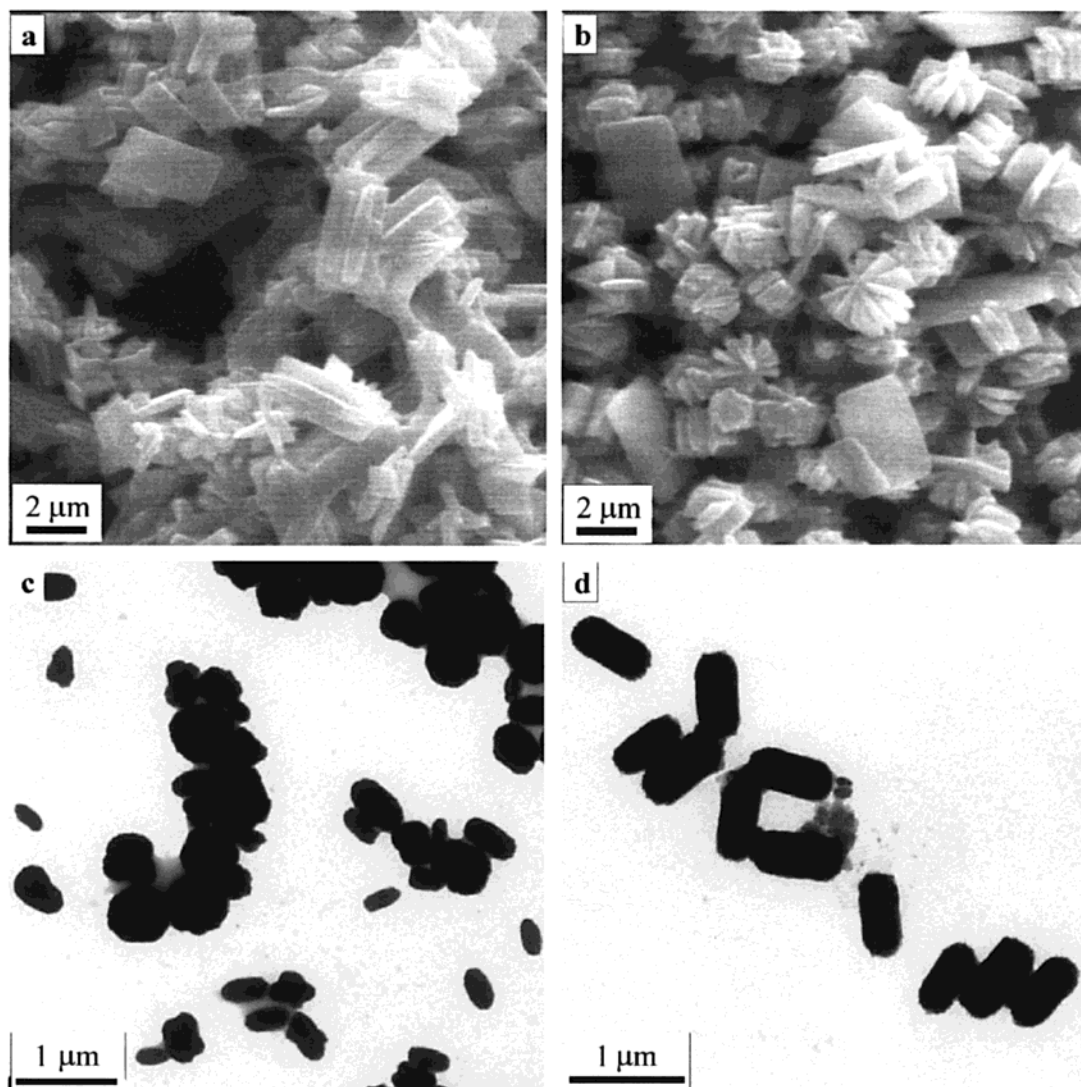
Figure 2. SEM (a, b) and TEM (c, d) micrographs of $BaSO_4$ particles obtained in the presence of PEG at pH 9 (a) and pH 5 (b), and PMAA at pH 9 (c) and pH 5 (d).

the products are well-crystallized barite crystals. However, unusual branched or nested crystals, which are not very uniform in both size and branch number, can be obtained at both pH 9 (Figure 2a) and pH 5 (Figure 2b). They seem to consist of aligned tablets, together with the normal rectangular tablets. This interesting result suggests that PEG does not exhibit a considerable inhibition effect on the barite crystallization, but it shows considerable influence on the crystal growth process of barite, possibly due to the presence of a specific weak interaction between PEG and growing $BaSO_4$ crystals.

In contrast, PMAA, a homopolymer carrying carboxylic acid groups, has shown a large inhibition effect on the barite crystallization. The solution did not become turbid until 180 and 50 min after the continuous addition of reactants at pH 9 and 5, respectively. The corresponding XRD results revealed that the products have a nanocrystalline barite structure with average crystalline sizes of 33 and 22 nm for samples obtained at pH 9 and 5, respectively. The particles obtained at pH 9 are a mixture of submicrometer-sized spheres and ovals (Figure 2c), whereas those obtained at pH 5 are rather uniform rodlike particles with an average size

of 0.8 μm and an aspect ratio of 2.1 (Figure 2d). The rodlike morphology implies that these particles could be formed by directional aggregation of rodlike nanocrystallites along the rod axes, resulting in a superstructure. The large inhibition effect of PMAA on the barite crystallization is not surprising because it is well known that the carboxylic acid groups of PMAA can interact strongly with many inorganic minerals. For example, a large inhibition effect of similar homopolymers on the crystallization of $CaCO_3$ [22,24] and ZnO [26] has been observed. Note that the delay time for the precipitation of $BaSO_4$ particles in the presence of PMAA at pH 9 is much longer than that at pH 5, indicating a stronger inhibition effect at a higher pH. This can be explained by considering that at a higher pH, the carboxylic acid groups of PMAA are more negatively charged and so interact more strongly with the growing $BaSO_4$ particles.

Barite Crystallization in the Presence of Double-Hydrophilic Block Copolymers Containing Carboxylic Acid Groups. Three different double-hydrophilic block copolymers containing carboxylic acid groups have been used for the controlled crystallization of $BaSO_4$. PEG-*b*-PMAA is a typical double-hydrophilic

block copolymer containing a strongly interactive carboxy-functionalized block, i.e., the PMAA block, which has been previously used in the controlled crystallization of calcium carbonate,[23,24] calcium phosphate,[25] and zinc oxide.[26] To examine the effect of pH on the barite crystallization in the presence of PEG-*b*-PMAA, we varied the pH value from 11 to 3. It was observed that the copolymer always showed a considerable inhibition effect for barite crystallization at a pH above 5; however, the onset of $BaSO_4$ precipitation and thus the inhibition effect gradually decreased from 90 to 40 min with decreasing pH from 11 to 5, in agreement with the results for PMAA reported above. No considerable inhibition effect was observed at pH 3 where the precipitation of $BaSO_4$ occurred sooner than 30 min, similar to the case without polymeric additives. The XRD results have shown that all of the products obtained at pH above 5 have a nanocrystalline barite structure with average nanocrystallite sizes ranging from 14 to 21 nm, whereas the product obtained at pH 3 exhibits well-crystallized barite crystals, which is consistent with the apparent observation on the inhibition effect.

Figure 3 shows the electron microscopy (EM) pictures of the obtained $BaSO_4$ particles. It can be observed that with decreasing pH from 11 to 5, the particle morphology essentially changes from ellipsoidal particles or ovals (pH 11) to peanuts (pH 9), a mixture of peanuts and single-notched spheres, i.e., peaches (pH 7), and peaches (pH 5), and the particle size gradually increases from around 0.65 to 2 μm. An enlarged picture shown in Figure 3c reveals the thorn-like surfaces of the peanut-like particles, suggesting a superstructure consisting of nanometer-sized rodlike subcrystals. The corresponding TG results show that the particles obtained at pH above 5 contain 4−9 wt % embedded polymer, consistent with their nanocrystalline structure. On the other hand, the $BaSO_4$ particles obtained at pH 3 are totally different and exhibit a mixture of rectangular tablets and branches (Figure 3f), very similar to the particles obtained in the presence of homopolymer PEG. The corresponding TG result reveals that no considerable amount of polymer is present.

The effect of pH on the barite crystallization in the presence of PEG-*b*-PMAA can be interpreted in terms of the influence of pH on the degree of the protonation of the carboxylic acid groups of the PMAA block. In the literature, the dissociation constant pK_a for poly(carboxylic acid) has been reported to be around 4.5.[36,37] Therefore, at pH above 5, the PMAA block is mainly in the form of polyanionic chains, resulting in a strong interaction between the PMAA block and the growing $BaSO_4$; thus, a large inhibition effect on the barite crystallization occurs, which becomes weaker with decreasing pH. Meanwhile, the PEG block is excluded from the crystallization surfaces because of its weak affinity for $BaSO_4$ and plays a role in preventing flocculation of crystals by steric repulsion. In contrast, at pH 3, the PMAA block is close to a neutral chain, resulting in a very weak interaction between the PMAA block and the growing $BaSO_4$, and thus little inhibition effect on the barite crystallization is found. Meanwhile,

the PEG block could interact directly with crystallizing surfaces and thus play an important role in controlling the crystal growth of barite, leading to the formation of barite morphologies similar to the case of homopolymer PEG.

Coupling aspartic acid to 27% of the carboxylic acid groups of the PMAA block of PEG-*b*-PMAA gives a copolymer with increased density of carboxylic acid groups, PEG-*b*-PMAA-Asp. The influence of PEG-*b*-PMAA-Asp on the barite crystallization is very similar to that of PEG-*b*-PMAA. The inhibition effect of PEG-*b*-PMAA-Asp was observed to be comparable to that of PEG-*b*-PMAA at both pH 9 and 5, and the XRD results also reveal a nanocrystalline barite structure with nanocrystallite sizes of 18 and 19 nm for $BaSO_4$ particles obtained at pH 9 and 5, respectively. As shown in Figure 4, most of the particles grown in the presence of PEG-*b*-PMAA-Asp at pH 9 are peanut-like particles with a mean length about 0.8 μm, whereas the particles produced at pH 5 are peach-like particles with an average size of 2.0 μm, which are more uniform than the particles obtained in the presence of PEG-*b*-PMAA at pH 5. The SEM image shown in Figure 4c more clearly suggests that these nearly spherical particles are not perfect spheres but peach-like spheres with single notches. Figure 4d presents a TEM image of a thin-section sample, which shows the presence of single notches in the peaches and reveals that the outer part of the peaches consists of rodlike nanocrystals that are radially aligned. The similarity in the influence of PEG-*b*-PMAA and PEG-*b*-PMAA-Asp on the barite crystallization sounds reasonable because both polymers have the same molecular backbone structure and the same functional groups that can strongly interact with $BaSO_4$ particles, i.e., the carboxylic acid groups. However, the modification with aspartic acid groups together with the consequent increase in the carboxylic group density may contribute to the small variation in the particle morphology.

PEG-*b*-PEIPA is another copolymer containing carboxylic acid groups and its interactive PEIPA block is essentially a poly-EDTA block that contains excellent chelate complexers for bivalent cations.[22,23] Similarly, the inhibition effect of PEG-*b*-PEIPA for barite crystallization was found to be comparable to that of PEG-*b*-PMAA at both pH 9 and 5, and the XRD results reveal a nanocrystalline barite structure with nanocrystallite sizes of 11 and 27 nm for $BaSO_4$ particles obtained at pH 9 and 5, respectively. However, there are significant differences in the particle morphology. In the presence of this polymer, ellipsoidal or oval-like particles with a mean size about 0.5 μm can be obtained at pH 9, whereas well-defined peanut-like particles with a mean length of 3.0 μm can be synthesized at pH 5 (Figure 5). The SEM picture shown in Figure 5c reveals the rough surfaces of the peanuts. The TEM image from a thin-section sample shows that the peanuts are composed of rodlike nanocrystals that are radially oriented from the revolutional axis of the peanut (Figure 5d). Note that although the particle size still increases with decreasing pH, the peanut-like particles are now obtained at pH 5 instead of pH 9 as in both cases of PEG-*b*-PMAA and PEG-*b*-PMAA-Asp. The number of the carboxylic acid groups in PEG-*b*-PEIPA is about 20, much larger than

(36) Chibowski, S. *J. Colloid Interface Sci.* **1990**, *140*, 444.
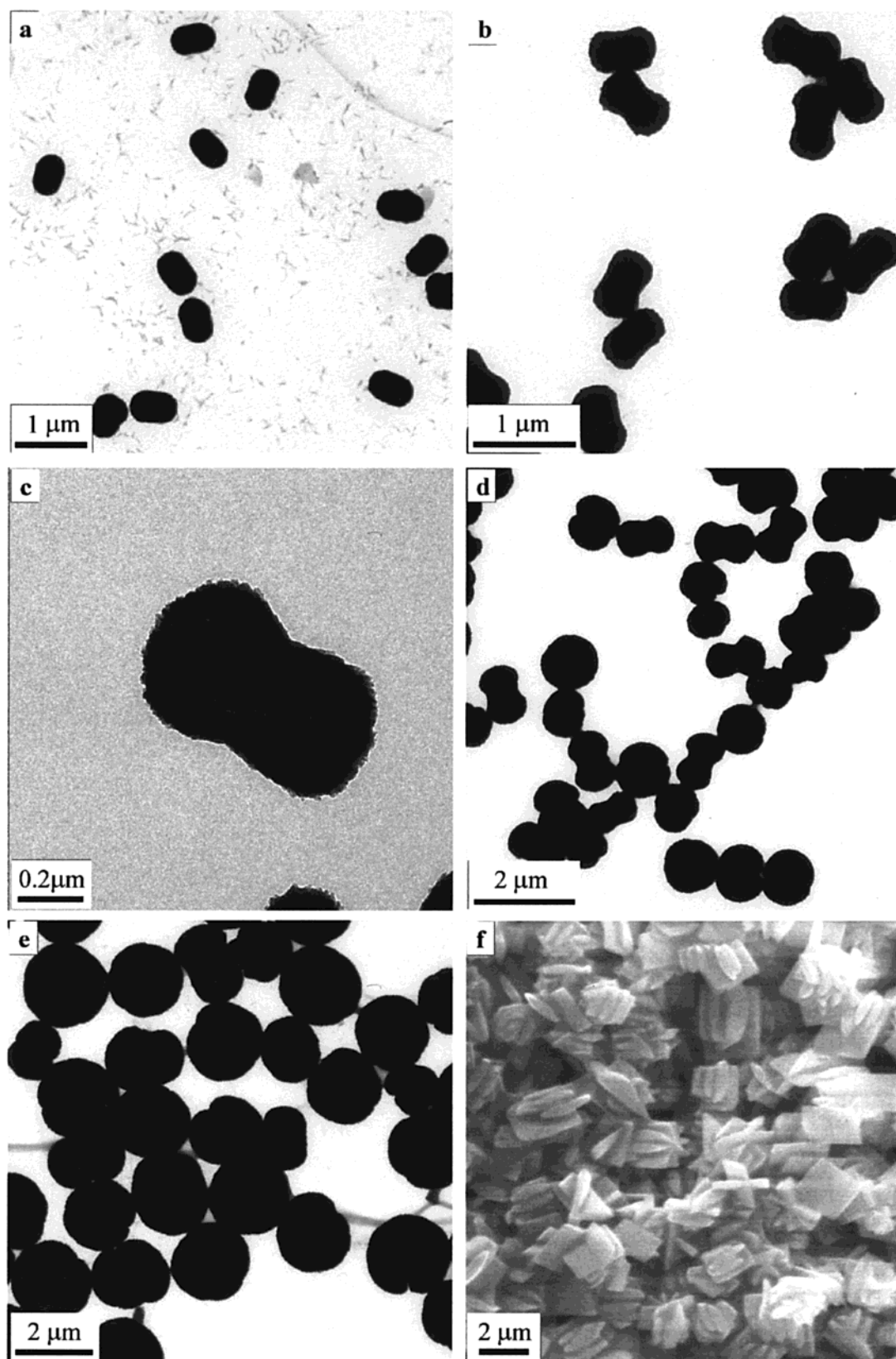(37) Zhang, S.; Gonsalves, K. E. *Langmuir* **1998**, *14*, 6761.

Figure 3. TEM (a−e) and SEM (f) micrographs of BaSO$_4$ particles obtained in the presence of PEG-*b*-PMAA at pH 11 (a), 9 (b, c), 7 (d), 5 (e), and 3 (f).

that in PEG-*b*-PMAA, for which it is only 6. Moreover, the PEIPA block, which is a poly-EDTA analogue containing excellent chelate complexers, would show much stronger interaction with BaSO$_4$ particles than the PMAA block that contains single carboxylic acid groups. Therefore, at the same pH and weight concen-

tration of polymer solutions, the interaction of the PEIPA block with growing BaSO$_4$ would be stronger than that of the PMAA block. Because the interaction increases with increasing pH, the interaction from the PEIPA block at a certain pH would be similar to that from PMAA at a higher pH. Considering the large
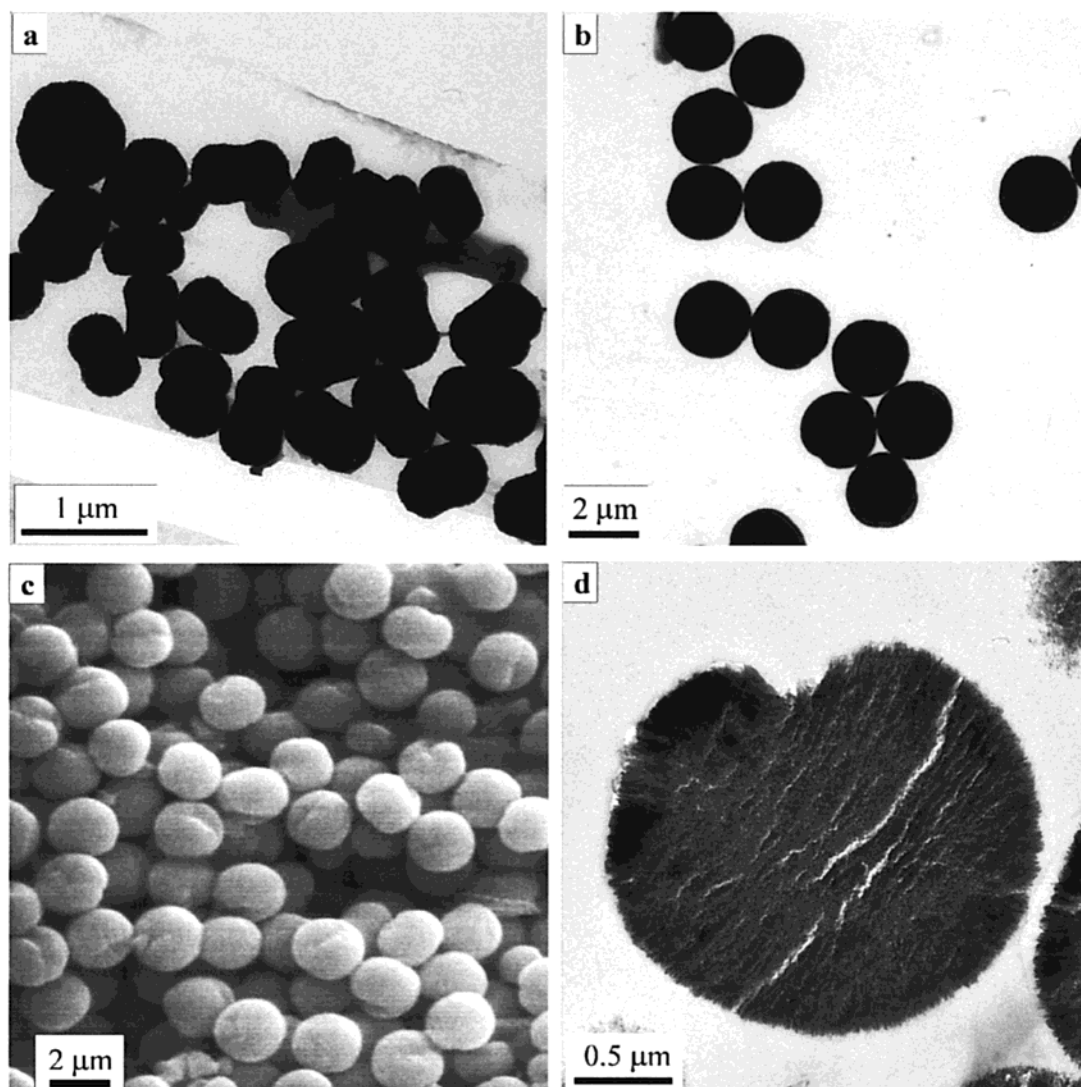
Figure 4. TEM (a, b, d) and SEM (c) micrographs of BaSO$_4$ particles obtained in the presence of PEG-*b*-PMAA-Asp at pH 9 (a) and 5 (b−d). The picture (d) is from a thin-section sample.

influence of such interaction on the morphology of BaSO$_4$ particles, the ovals and peanuts obtained in the presence of PEG-*b*-PEIPA at pH 9 and 5 could essentially correspond to the ovals and peanuts obtained in the presence of PEG-*b*-PMAA at pH 11 and 9, respectively. The difference in the molecular structure and conformation of the copolymers could also contribute to the difference in the size and morphology of the final particles.

Note that peanut-like hematite (α-Fe$_2$O$_3$) particles with very similar shape and size have been produced by a gel−sol method in the presence of sulfate ions.[38−40] It has been disclosed that the bidentate-specific adsorption of sulfate ions to the growing surfaces parallel to the *c* axis resulted in the formation of hematite nanorods.[41] The mechanism of the formation of the peanutlike shape has been explained in terms of the gradual outward bending of the dense rodlike subcrystals or

nanorods on both ends of an ellipsoidal particle by the growth of new crystalline nanorods in the spaces between the existing subcrystals.[40] Such a growth process has already been strongly supported by recent computer simulation results.[42] In the present case, it can be reasonably assumed that the carboxylic acid groups of PEG-*b*-PEIPA could be preferentially adsorbed on the growing surfaces parallel to a certain crystallographic direction of barite, resulting in rodlike nanocrystals. Peanut-like barite particles could be formed in a way similar to the case of peanut-like hematite particles, i.e., through the outward bending of adjoining subcrystals by nucleation and growth of a new subcrystal in each space between them. Such a growth mechanism may also be applied to the formation of peanutlike particles for both PEG-*b*-PMAA and PEG-*b*-PMAA-Asp, where the PMAA and PMAA-Asp blocks would play a role similar to the role the PEIPA block plays, although the obtained peanuts in the latter cases are much smaller and less uniform.

It is noteworthy that all of the barite particles obtained in the presence of the three copolymers con-

(38) Sugimoto, T.; Khan, M. M.; Muramatsu, A. *Collds Surf. A* **1993**, *70*, 167.

(39) Sugimoto, T.; Khan, M. M.; Muramatsu, A.; Itoh, H. *Colloids Surf. A*, **1993**, *79*, 233.

(40) Shindo, D.; Park, G.-S.; Waseda, W.; Sugimoto, T. *J. Colloid Interface Sci.* **1994**, *168*, 478.

(41) Sugimoto, T.; Wang, Y. *J. Colloid Interface Sci.* **1998**, *207*, 137.

(42) Sasaki, N.; Murakami, Y.; Shindo, D.; Sugimoto, T. *J. Colloid Interface Sci.* **1999**, *213*, 121.
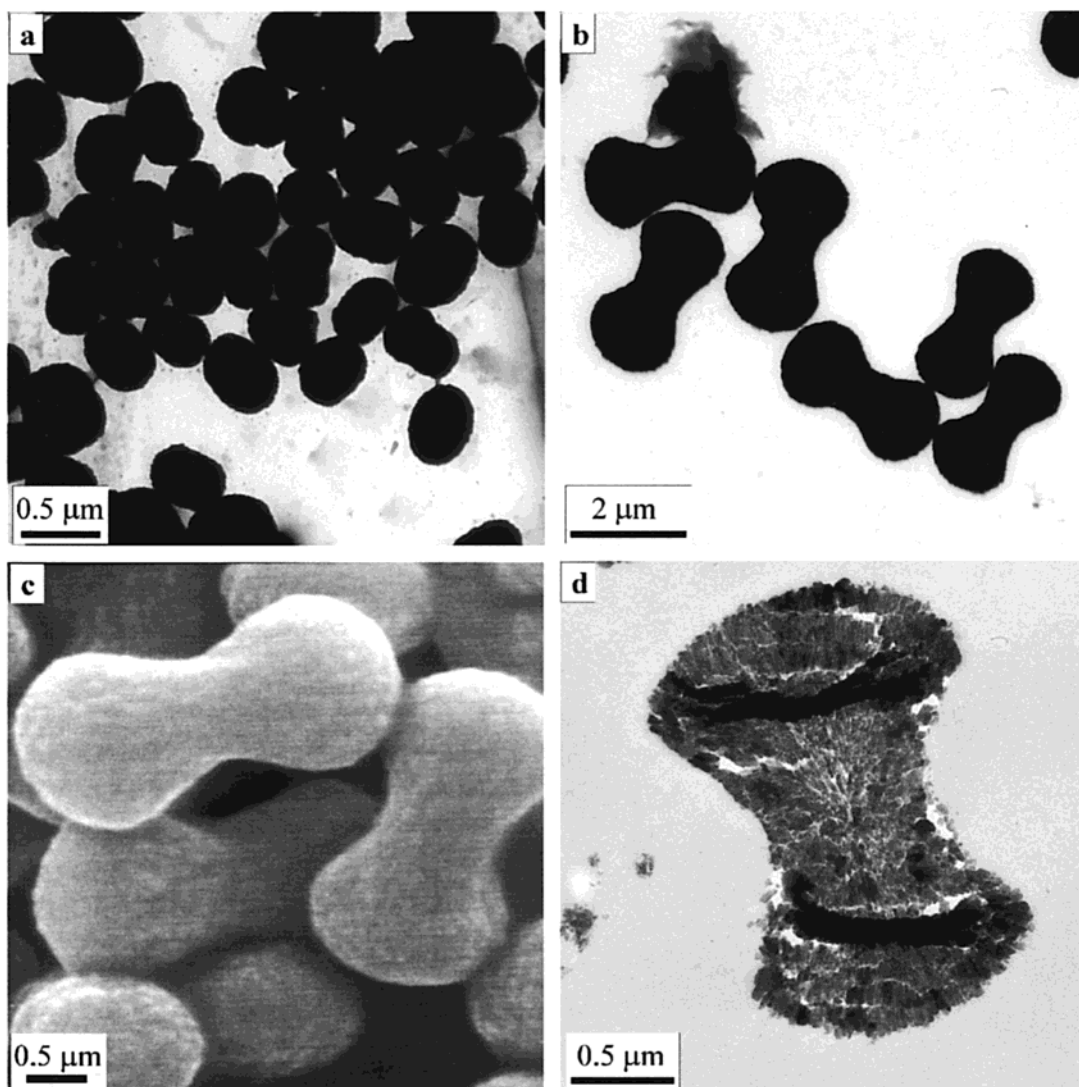
Figure 5. TEM (a, b, d) and SEM (c) micrographs of BaSO$_4$ particles obtained in the presence of PEG-*b*-PEIPA at pH 9 (a) and 5 (b−d). The picture (d) is from a thin-section sample.

taining carboxylic acid groups at pH above 5 exhibit a nanocrystalline structure and are very likely composed of rodlike nanocrystals that act as building blocks or subcrystals. It is very interesting to note that there exists a general trend in the morphology variation of barite particles in the presence of all the copolymers containing carboxylic acid groups with decreasing pH from 11 to 5, i.e., from ovals to peanuts, and then to peaches. A progressive growth of fluorapatite aggregates in a gelatin matrix from rods to peanuts, dumbbells, notched spheres, and finally spheres has been reported.[15] The fractal branching of successive generations, which results in the morphogenesis of the fluorapatite spheroids, together with the overall symmetry of the self-assembled aggregates has been considered to be a consequence of intrinsic electric fields, which take over control of aggregate growth. Accordingly, we can also assume that the ovals, peanuts, and peaches represent different stages of the directed aggregation of barite nanorods in a similar process, where the peanut shape basically represents the field lines of a dipole field of a primary rodlike aggregate and further growth at the caps of the peanut structure would yield spheres with notches such as peaches. However, a

shortcoming for this explanation lies in that these particles do not necessarily represent different stages of a single growth process. Moreover, the TEM micrographs from thin-section samples for the peach-like particles (Figure 4d) have not clearly shown an alignment of the rodlike nanocrystals along field lines or a strict fractal structure. Specifically, the torus-shaped cavity around the elongated seed, which has been clearly observed for the fluorapatite spheroaggregate and successfully simulated by assuming a fractal model,[15] cannot be seen in the present case. Therefore, the morphogenesis of the barite aggregates seems not exactly the same as that of the fluorapatite aggregates, even though they apparently exhibit very similar morphologies.

Another possible interpretation is to assume that the probability of nucleation on the side-surfaces of rodlike or ellipsoidal primary particles plays an important role in determining the final morphology of BaSO$_4$ particles. If no nucleation on the side-surfaces occurs, rodlike subcrystals can only attach to each other side-by-side and end-by-end, resulting in rodlike or oval-like particles (Figure 6a). If there is a certain degree of nucleation probability on the side-surfaces, the outward
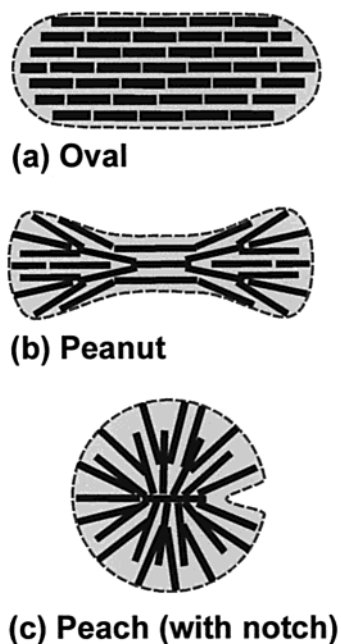
Figure 6. Schematic growth mechanisms of oval-, peanut-, and peach-like BaSO$_4$ particles: without side-surface nucleation (a), with side-surface nucleation and growth at limited tilt angles (b), and with side-surface nucleation and growth at random tilt angles (c).

bending of adjoining subcrystals can be achieved by nucleation and growth of new subcrystals on the side-surfaces of pre-existing subcrystals at limited tilt angles, resulting in peanut-like particles (Figure 6b). Finally, if the nucleation probability on the side-surfaces is so large that nucleation and growth on side-surfaces can occur at random tilt angles, spherical particles including notched spheres would tend to form (Figure 6c). The nucleation probability on side-surfaces would become larger if the binding interaction of polymers on the side-surfaces of rodlike barite nanocrystals becomes weaker. Because the intensity of binding interaction of copolymers containing carboxylic acid groups decreases essentially with decreasing pH, the nucleation probability on side-surfaces would increase with decreasing pH, leading to the observed variation trend of the particle morphology from ovals to peanuts, and then to peaches with decreasing pH till pH = 5. However, the mechanism of the formation of peaches instead of perfect spheres remains to be elucidated. It is also noteworthy that only rodlike particles can be obtained in the presence of homopolymer PMAA even at pH 5, which suggests that the presence of a solvating PEG block in the copolymers could contribute to the formation of peaches or peanuts.

Although the origins of peanuts and peaches remain to be unequivocally elucidated, it seems clear that there are two main points accounting for their formation, i.e., the formation of rodlike subcrystals and the outward bending of adjoining subcrystals. For homopolymer PMAA, the preferential adsorption of the homopolymer containing COOH groups on selected crystal faces leads to the formation of rodlike subcrystals, but the outward bending of adjoining subcrystals is not favored, resulting in the final rodlike aggregates. In contrast, the presence of a second, nonadsorbing PEG block would play the role of a spacer, which is present between the growing

subcrystals jostling one another, and so would enhance the outward bending of the subcrystals, favoring the formation of peanuts and peaches. It appears that the combination of the interacting PMAA block, which can be preferentially adsorbed on selected crystal faces, and the noninteracting PEG block, which acts both as a solvating block and an effective spacer, makes these double-hydrophilic block copolymers work well in controlling barite morphology and become a potential effective morphology controller of many other inorganic materials.

Barite Crystallization in the Presence of a Double-Hydrophilic Block Copolymer Containing Phosphonate Groups. It is well known that (poly)phosphonate-type additives are very effective inhibitors for the barite crystallization due to the strong interaction between the phosphonate groups and the growing BaSO$_4$ crystals.[31,32,43] Partial phosphonation (21%) of the carboxylic groups of PEG-b-PMAA produces a copolymer containing phosphonate groups (PEG-b-PMAA-PO$_3$H$_2$), which is expected to exhibit an even larger inhibition effect on the barite crystallization than that of PEG-b-PMAA.

Indeed, the precipitation of BaSO$_4$ did not occur until 150 min in the presence of PEG-b-PMAA-PO$_3$H$_2$ at pH 9, much later than the onset (75 min) of the BaSO$_4$ precipitation in the presence of PEG-b-PMAA at the same pH. The XRD result shows that the resulting product exhibits a nanocrystalline structure with an average crystallite size of 11 nm. The TEM micrograph shown in Figure 7a shows that the product consists of a large number of fluffy spherical particles (0.3−0.5 μm) and a few long fibers. Figure 7b reveals that the obtained fibers are essentially bundles of nanofilaments ranging from 20 to 30 nm in diameter. The particle showing short tails (Figure 7c) seems to represent the earlier stage of the long bundle of nanofilaments with a single starting point (Figure 7d), strongly indicating that the fibers could be formed by nucleation at single points followed by crystal growth along a preferred crystal direction.

Pure bundles of barite nanofilaments can be produced in the presence of PEG-b-PMAA-PO$_3$H$_2$ at pH 5, where macroscopic crystal formation was not observed until 180 min and the product was composed of relatively well crystallized barite with an average crystallite size about 60 nm in the (211) direction according to the corresponding XRD result. The SEM micrograph (Figure 8a) clearly shows the presence of bundles of filaments, the lengths of which are considerably varied and can be as large as more than 100 μm. It is noteworthy that almost all the bundles of fibers have their single starting points. Various appearances such as snails, bananas, and cones can be observed. Figure 8b presents a typical TEM micrograph of the bundles of fibers, which suggests that these fibers essentially consist of bundles of nanofilaments that are rather uniform in diameter (20−30 nm). Figure 8c presents a typical TEM image of a thin section of a bundle of BaSO$_4$ nanofilaments sliced nearly along the fiber axis, which shows a large area of long continuous nanofilaments that exhibit rather uniform diameters (20−30 nm) and are aligned approximately par-

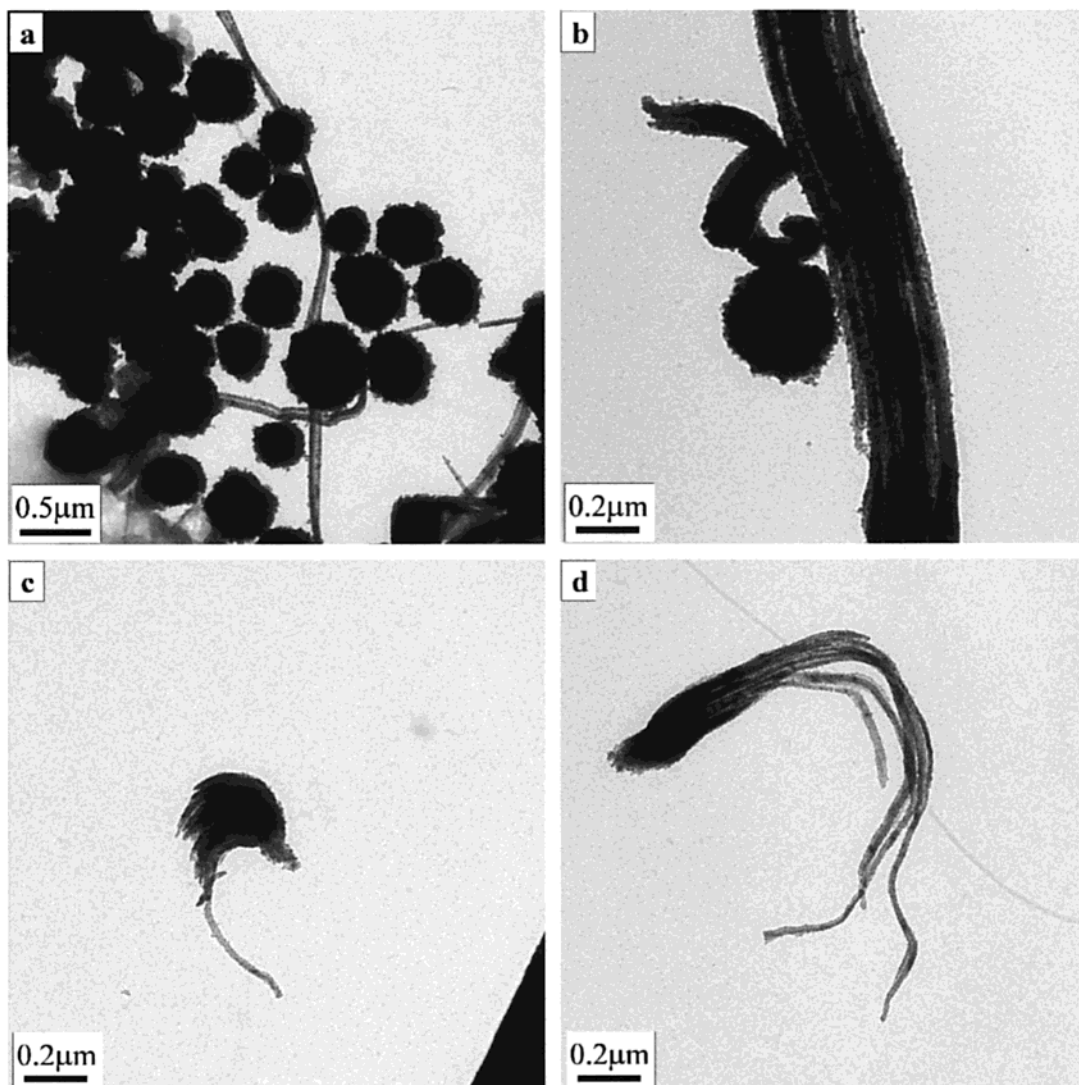(43) Leeden, M. C.; Rosmalen, G. M. *J. Colloid Interface Sci.* **1995**, *171*, 142.

Figure 7. TEM micrographs of BaSO$_4$ particles obtained in the presence of PEG-*b*-PMAA-PO$_3$H$_2$ at pH 9.

allel to each other. The corresponding electron diffraction pattern consists of elongated but individual diffraction spots, most of which can be indexed as the reflections corresponding to the [001] zone of barite. It can be seen that the (210) reflection is located along the direction exactly normal to the filament axis, suggesting that each nanofilament is a single crystal elongated along the crystallographic [1$\bar{2}$0] axis. It is noteworthy that a few reflections corresponding to other zones are also present in the whole diffraction pattern due to a minor degree of rotation of some filaments along their own filament axes. Specifically, reflections (211) and (221) accompany reflections (210) and (220), respectively. The observation that the (211) reflection is also located along the direction almost normal to the filament axis confirms that the filaments are elongated along the crystallographic [1$\bar{2}$0] axis. The absence of symmetry respective to the [1$\bar{2}$0] axis in the diffraction pattern indicates that the individual nanofilaments in one bundle cannot be randomly rotated along their filament axes. Instead, these nanofilaments are vectorially aligned, i.e., either geometric packing or force fields result in a high degree of correlation between the fibers with respect to the crystallographic direction. The fact that the nanofilaments are elongated along the [1$\bar{2}$0] axis indicates that the phosphonated copolymer preferentially adsorbs on the crystalline faces parallel to the [1$\bar{2}$0] axis, such as the faces (001), (210), and (211). A typical TEM image of a thin section of a bundle of BaSO$_4$ nanofilaments sliced nearly perpendicular to the fiber axis shown in Figure 8d shows that the nanofilaments constituting a bundle are not aligned very densely and there are some empty spaces between each nanofilament, which could be filled by the incorporated copolymers. This observation is consistent with the corresponding TG result, which reveals that these hybrids show a rather large polymer content (8.8 wt %).

The formation of bundles of barite nanofilaments could be attributed to the strong and specific interaction between the phosphonate groups of the copolymer and the crystallizing BaSO$_4$ particles, which results in the large inhibition effect on the barite crystallization and the preferential adsorption of the polymer on the crystal surfaces parallel to the crystallographic [1$\bar{2}$0] direction. It has been observed that only a very small amount of fibers was formed when the injection of reactants was stopped at 180 min, and the majority of fibers formed gradually under static conditions. This finding indicates that a metastable, inhibited BaSO$_4$ species was kept in solution at rather high concentrations due to the strong
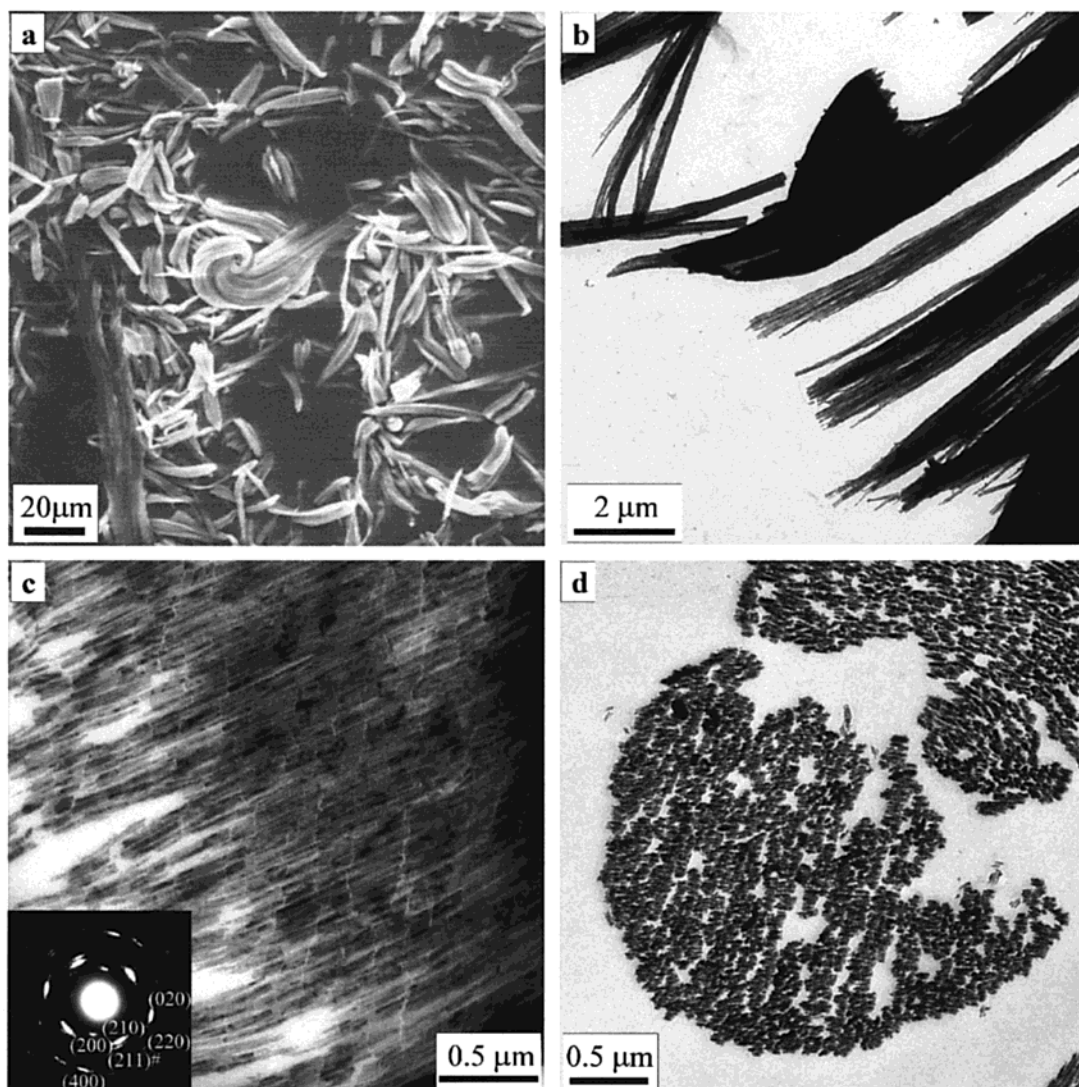
Figure 8. SEM (a) and TEM (c−d) micrographs of BaSO₄ particles obtained in the presence of PEG-*b*-PMAA-PO₃H₂ at pH 5. The pictures (c, d) are from thin-section samples. Inset in (c) shows the corresponding electron diffraction pattern. Except the reflections labeled "#", all indexed reflections correspond to the [001] zone of barite.

inhibition effect of the copolymer. Anisotropic crystal nuclei could be formed from these BaSO₄ species by heterogeneous nucleation either on the surfaces of the reactor or the connection point between the two reactant jets before the injection of reactants was stopped, or on the surfaces of the container after the injection of reactants was stopped. Subsequently, the inhibited BaSO₄ species were added slowly on the existing anisotropic nuclei, which acted as starting points, causing the nuclei to grow into bundles of crystalline nanofilaments elongated along the crystallographic [1$\bar{2}$0] direction due to the preferential adsorption of the phosphonated copolymer on the crystal surfaces parallel to the crystallographic [1$\bar{2}$0] direction. However, if the inhibition effect on the barite crystallization is so strong that the heterogeneous nucleation necessary for the fiber growth is significantly prevented (as at pH 9), a large number of fluffy particles may form suddenly when the concentration of inhibited BaSO₄ species exceeds a certain value. It would be very interesting to investigate the time evolution of these bundles of nanofibers to elucidate the growth mechanism. Such a study is underway and will be reported in due time.

It is noteworthy that BaSO₄ nanofilaments have also been synthesized in reverse microemulsions consisting of a continuous oil phase and water droplets stabilized by the surfactant Aerosol OT (AOT).[30] In that case, the nanofilaments were also formed by a slow growth process under static conditions. However, usually single nanofilaments instead of bundles of nanofilaments were formed and the nanofilaments were found to be elongated along the crystallographic [010] axis that is different from the [1$\bar{2}$0] axis observed in the present case. These differences may be attributed to the difference in the specific interaction of the surfactant AOT and the phosphonated copolymer with the growing BaSO₄ in the corresponding reaction media.

Theoretical calculation of the surface energies of barite has revealed that the surfaces parallel to [1$\bar{2}$0], such as (001), (210), and (211), are the lowest energy surfaces of barite.[44,45] The preferential adsorption of the

(44) Allan, N. L.; Rohl, A. L.; Gay, D. H.; Catlow, R. A.; Davey, R. J.; Mackrodt, W. C. *Faraday Discuss.* **1993**, *95*, 273.
(45) Redfern, S. E.; Parker, S. C. *J. Chem. Soc., Faraday Trans.* **1998**, *94*, 1947.

phosphonated copolymer on these faces suggests the possible presence of specific stereochemical or geometric association between the interactive phosphonated block and the most stable surfaces of barite. However, it has been shown that the adsorption behavior of polyelectrolytes on barite is very complex due to the presence of various factors including the extent of adsorption, the strength of attachment, and the adsorption rate, and the specific structural matching seems not necessarily present between a polymer and a barite surface with which it interacts strongly.[43] Because the phosphonated block copolymer used here has a much more complex structure, it seems not yet possible to clearly identify if there is any specific structural matching present in the adsorption process. Although molecular modeling techniques have been successfully used to investigate the interaction of low-molecular-weight diphosphonates with the barite surfaces,[33] their application still remains to be extended to polymeric additives. Recently, molecular dynamics calculations have been used for the interaction of polymeric additives with $CaCO_3$ (calcite) surfaces, but the interplay between various competitive effects makes the adsorption process very complex and it is not yet possible to unequivocally relate the chemical structures of the polymers to their different adsorption behavior.[46] It is clear that much effort is required to investigate and elucidate the specific interaction between these phosphonated block copolymers and the barite surfaces, which would account for the preferential adsorption of the polymer on the surfaces parallel to [1$\bar{2}$0].

Conclusions

Double-hydrophilic block copolymers consisting of a binding block and a solvating block have been used as very effective crystal growth modifiers to direct the controlled synthesis of barite particles with unusual and well-defined morphologies. Such $BaSO_4$ particles with various morphologies are promising candidates for materials science due to the importance of shape and texture in determining various properties of materials.[1] The influences of variation in functional group and molecular structure of the copolymers as well as variation of pH condition on the particle size and morphology have been examined in detail. The obtained results shed some new light on the understanding of crystal-additive interactions that could be applied to many other systems. The formation of the different types of inorganic morphologies in the presence of different functional polymeric patterns at room temperature extends the possibilities of previous attempts of inorganic morphogenesis,[2] which usually employs surfactant assemblies as supramolecular templates. Compared with simple surfactants, block copolymers containing polyanionic groups are more like the protein macromolecules that are present in organisms to exert control over the biomineral growth[9–11] and are expected to enable more elaborate control of crystal morphology and structure. Specifically, complex patterns of chemical groups can be established by varying the binding and solvating blocks in double-hydrophilic block copolymers according to molecular design, leading to still more specific tools for the controlled formation of hybrid superstructures with complex architectures.

CM0010405

(46) Hadicke, E.; Rieger, J.; Rau, I. U.; Boeckh, D. *Phys. Chem. Chem. Phys.* **1999**, *1*, 3891.